ACS Sustainable Chemistry & Engineering

Research Article

pubs.acs.org/journal/ascecg

Flame Retardant, Heat Insulating Cellulose Aerogels from Waste Cotton Fabrics by in Situ Formation of Magnesium Hydroxide Nanoparticles in Cellulose Gel Nanostructures

Yangyang Han, Xinxing Zhang,* Xiaodong Wu, and Canhui Lu*

State Key Laboratory of Polymer Materials Engineering, Polymer Research Institute of Sichuan University, Chengdu 610065, China

Supporting Information

ABSTRACT: Cellulose aerogels with low density, high mechanical strength, and low thermal conductivity are promising candidates for environmentally friendly heat insulating materials. The application of cellulose aerogels as heat insulators in building and domestic appliances, however, is hampered by their highly flammable characteristics. In this work, flame retardant cellulose aerogels were fabricated from waste cotton fabrics by in situ synthesis of magnesium hydroxide nanoparticles (MH NPs) in cellulose gel nanostructures, followed by freeze-drying. Our results demonstrated that the three-dimensionally nanoporous cellulose gel prepared from the NaOH/urea solution could serve as scaffold/template for the nonagglomerated growth of MH NPs. The prepared hybridized cellulose aerogels showed excellent flame retardancy, which could extinguish within 40 s. Meanwhile, the thermal conductivity of the composite aerogel increased moderately from 0.056 to 0.081 W m^{-1} k^{-1} as the specific surface area decreased slightly from 38.8 to 37.6 cm^2 g^{-1}, which indicated that the excellent heat insulating performance of cellulose aerogel was maintained. Because the concepts of the process are simple and biomass wastes are sustainable and readily available at low cost, the present approach is suitable for industrial scale production and has great potential in the future of green building materials.

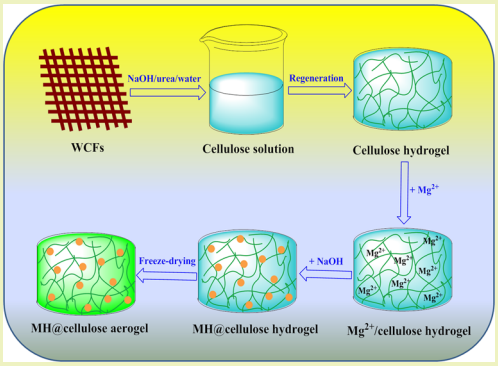

KEYWORDS: *Cellulose aerogel, Flame retardant, Heat insulating, Waste cotton fabrics, Template*

INTRODUCTION

In recent years, large volumes of waste cotton fabrics (WCFs) were produced annually by the manufacture of clothing and other textile products.[1] Used clothes and leftover materials of the textile industry are usually landfilled or incinerated.[2] These disposing methods caused two major problems: waste of valuable cotton resources and environmental pollution. Hence, it is an attractive and viable attempt to recycle WCFs or other biomass wastes[3−5] into value-added products for both environmental and economic benefits. A number of methods have been reported about recycling WCFs. Ratanakamnuan et al. prepared cellulose esters from WCFs under microwave activation, which did not change the chemical structure of the esterified cellulose.[6] Tian et al. developed a mechanochemical method to prepare carboxylate-functionalized cellulose from WCFs for the removal of cationic dyes from aqueous solutions.[7] Sun et al. extracted microcrystalline cellulose by hydrolyzing WCFs and introduced it into poly(vinyl alcohol) for promoting the melt-processability of this composites.[8] Hong et al. reported that WCFs pretreated with ionic liquid have a potential to serve as a high-quality carbon source for bacterial cellulose production.[9] However, none of these methods have been translated into commercial application due to the high processing cost. Until now, the large scale and effective conversion of WCFs into value-added products is still a challenge for the textile industry and environmental engineers.

One potential way to add value utilizing WCFs is preparing cellulose aerogels from WCFs and use them as thermal insulating materials for building or domestic application (e.g., refrigerator insulation material).[10] Cellulose aerogels with low density, excellent mechanical properties, large surface area, and ease of modification have recently emerged as a new class of advanced materials.[11] It can be manufactured from biomass wastes by using a very cheap NaOH/urea aqueous solution.[12] This renewable and environmentally friendly material has been used in various applications, such as flexible electronic devices,[13] catalyst support,[14] wastewater treatment,[15] prototype for carbon aerogel production,[16] and so on. Cellulose aerogel is considered as one of the most promising thermal insulating materials due to its abundant internal pores and good heat insulation performance.[10,17] However, cellulose aerogel is easy to ignite, which makes it impossible to be used as building materials or domestic appliances. Therefore, the flame retardant modification of cellulose aerogel is crucial for expanding the application field of this advanced material, but it remains a

Received: May 16, 2015
Revised: June 18, 2015
Published: July 2, 2015

DOI: 10.1021/acssuschemeng.5b00438
ACS Sustainable Chem. Eng. 2015, 3, 1853−1859

challenge. The main obstacle is how to realize fine dispersion of flame retardants in the high viscosity cellulose solution and avoid the collapse of the three-dimensionally nanoporous structures with the addition of abundant inorganic fillers.

Instead of the traditional mixing of flame retardants in a polymer matrix, we propose a new approach using three-dimensionally nanoporous cellulose gels prepared by dissolution and coagulation of cellulose from aqueous NaOH/urea solution as templates for the nonagglomerated growth of magnesium hydroxide nanoparticles (MH NPs).[18−20] The resulting composite gels were freeze-dried to prepare aerogel with a low density, high mechanical properties, excellent flame retardancy, and heat insulation. Through this facile and green approach, we successfully addressed the agglomeration of flame retardants in cellulose matrix, as well as the collapse of the three-dimensionally nanoporous structures of cellulose aerogels. This eco-friendly method for the preparation of cellulose-based flame retardant aerogels nanocomposites from WCFs not only reduces the WCFs pollution but also promotes the application of cellulose aerogels in heat insulating materials.

MATERIALS AND METHODS

Materials. Waste cotton fabrics (WCFs) without further purification or bleaching were collected from tailoring workshops and subjected to cutting and shredding processes. Sodium hydroxide, urea sulfuric acid, and magnesium chloride hexahydrate were purchased from Chengdu Kelong Chemical Plant and used without further purification.

Synthesis of MH NPs@Cellulose Composite Aerogels. The schematic of the preparation process for MH NPs@cellulose composite aerogels is shown in Figure 1. Initially, WCFs were

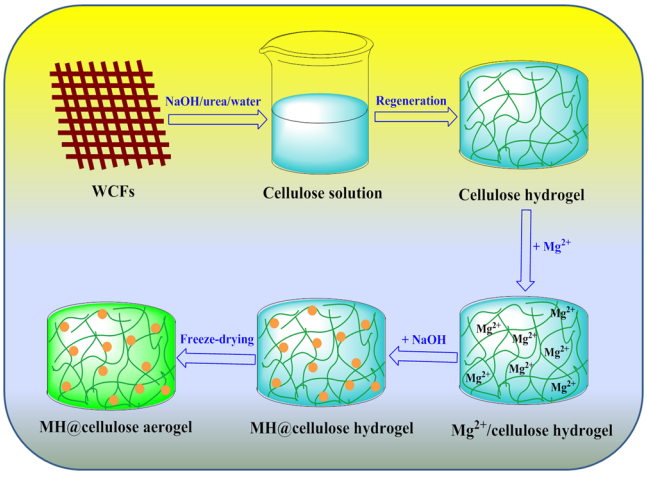

Figure 1. Schematic illustration of the in situ synthesis of MH NPs@cellulose composite aerogel.

smashed into pieces, and 100 g of aqueous solution with 7 wt % NaOH and 12 wt % urea was precooled to −12 °C in a refrigerator, which is proposed as a promising candidate for cellulose dissolution owing to its low cost, nontoxicity, and environmental friendliness.[21] Subsequently, 2 g (2 wt %) of WCFs was added immediately to the precooled solvent and stirred vigorously for 5 min at ambient temperature. After degasification, the viscous cellulose solution was casted, coagulated in 5 wt % H_2SO_4, and regenerated for 12 h at room temperature forming cellulose hydrogel with a three-dimensional cellulose fibrillar network nanostructure. The resulting cellulose hydrogels were washed with running water and deionized water to remove all soluble substances. Then, cellulose hydrogels were immersed into the magnesium chloride solution of various concentrations (0.25, 0.5, 0.75, and 1.0 mol/L) for 24 h. The obtained cellulose hydrogel containing Mg^{2+} were dipped in excess sodium hydroxide to synthesize MH NPs. The resultant MH NPs@cellulose composite hydrogels were washed with deionized water to remove the residual chemical reagents. Afterward, lyophilization of the frozen mixture took place within a freeze-drier apparatus at −54 °C under vacuum for 24 h. The removal of water phase in the composite hydrogel resulted in a porous nanostructure. Thus, a three-dimensional porous MH NPs@cellulose composite aerogel was obtained. Aerogels with different MH NPs loadings were coded as CA1, CA2, CA3, and CA4 in order to distinguish with the aerogel without MH NPs, which was coded as CA0. In other cases, the viscous cellulose solution was directly added with an appropriate amount of magnesium hydroxide to synthesize the composite aerogel.

Characterization. The morphology of the sample was observed by scanning electron microscope (SEM, JEOL JSM-5600, Japan) and transmission electron microscope (TEM, JEOL JEM-100CX, Japan) equipped with energy dispersive X-ray spectroscopy (EDS). X-ray diffraction (XRD) patterns were recorded on a Philips Analytical X'Pert X-diffractometer (Philips Co., The Netherlands) with Cu Kα radiation (λ = 0.1540 nm) at 40 kV and 30 mA in the range of 5−80° at room temperature. The specific surface area was determined by N_2 sorption at 77 K with automatic adsorption apparatus (Quantachrome Instruments, NOVA2000e). Thermogravimetric analysis (TGA) measurement was performed from room temperature to 700 °C with a heating rate of 10 °C/min under steady nitrogen on a TG209 F1 instrument (NETZSCH Co., Germany). MH NPs content of the composite aerogel was calculated by weighing the sample and neat cellulose aerogel. Density of the aerogel was calculated by weighing the sample and measuring its volume. Porosity of the aerogel was calculated according to the eq $(1 - \rho^*/\rho) \times 100\%$, where ρ^* is the density of the MH NPs@cellulose composite aerogel and ρ is theoretical density of cellulose.[22] The thermal conductivity of aerogels was measured by the transient plane source method (Hot Disk 2500, Sweden). The compressive strength of aerogels (diameter of 20 mm and height of 10 mm) was measured on an Instron 5567 universal testing machine at a compression speed of 1 mm/min. The flame retardant properties were evaluated by the measurement of combustion velocity within 10 s (50 mm × 10 mm × 3 mm). The samples of neat cellulose aerogel and MH NPs@cellulose composite aerogels (CA2) were used for SEM, TEM, XRD, TGA, and N_2 sorption measurements.

RESULTS AND DISCUSSION

Characterization of MH NPs@Cellulose Composite Aerogels. The XRD patterns are shown in Figure 2, which

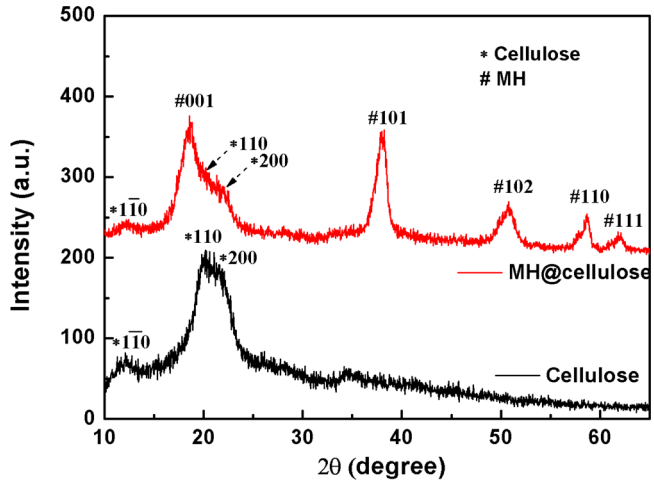

Figure 2. XRD patterns of neat cellulose aerogel and MH NPs@cellulose composite aerogel (CA2).

DOI: 10.1021/acssuschemeng.5b00438
ACS Sustainable Chem. Eng. 2015, 3, 1853−1859

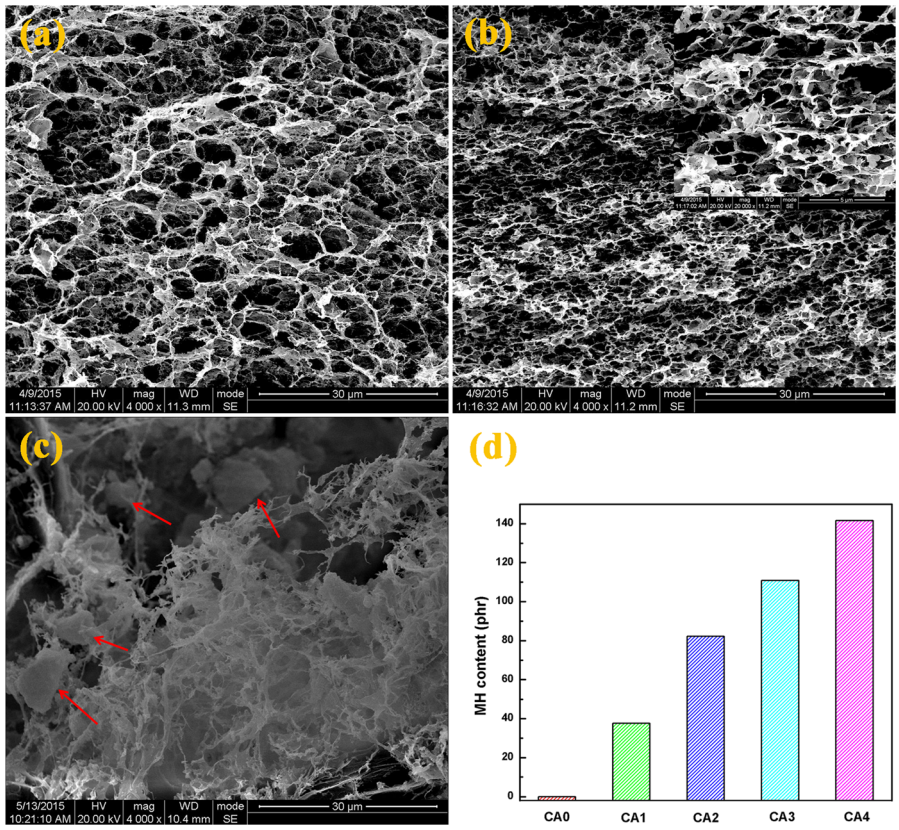

Figure 3. SEM images of (a) neat cellulose aerogel (scale bar: 30 μm), (b) MH NPs@cellulose composite aerogel (CA2) (scale bar: 30 μm, 5 μm for inset), and (c) directly mixed MH NPs-cellulose composite (scale bar: 30 μm), (d) MH NPs content in the composite aerogels (phr: parts per hundred parts of cellulose).

depict the crystal structure of the neat cellulose aerogel and MH NPs@cellulose composite aerogel. The diffraction peaks at 2θ = 12°, 20°, and 22° for (11-0), (110), and (200) planes are characteristic of cellulose II crystal.[23] The peaks located at 18.6°, 38.2°, 50.7°, 58.7°, and 61.8°, corresponding to the (001), (101), (102), (110), and (111) lattice planes, respectively, indicate the successful synthesis of the hexagonal structure MH NPs (JCPDS file number 7-239).[24] Furthermore, there is no sign of the disappearance of the characteristic peaks of cellulose and MH NPs, which indicates no interference in structure formation between the two components. However, the intensity of characteristic peaks of cellulose II decrease and peaks of (110) and (200) manifest as shoulder peaks compared to the neat cellulose aerogel. These might be the result of the incorporation of MH NPs into the cellulose aerogel. The coexistence of the cellulose and MH NPs peaks indicated that the MH NPs@cellulose composite aerogel was prepared successfully.

The structure and morphology of neat cellulose aerogel and MH NPs@cellulose composite aerogel were characterized by SEM and are shown in Figure 3a and b. Meanwhile, the MH NPs content was measured by the weighing method and is shown in Figure 3d. The neat cellulose aerogel displays a homogeneous porous structure (Figure 3a). The pore structure results from the sublimation of frozen water during the freeze-drying process.[22] The MH NPs@cellulose composite aerogel also exhibits a homogeneous porous structure even with the incorporation of a large amount (approximately 82 phr; parts per hundred parts of cellulose) of MH NPs (Figure 3b), which reveals that MH NPs did not have a remarkable influence on the nanoporous structure of cellulose aerogels by this in situ synthesis method. With high-magnification SEM, the magnesium hydroxide nanoparticles can be observed in the composite aerogel (Figure S1, Supporting Information). In contrast, as shown in Figure 3c, the MH-cellulose composite with 82 phr of MH content prepared by the directly mixing method does not has a homogeneous porous structure due to the collapse and blockage of the nanoporous structure with the agglomerate MH NPs. This could be explained that the agglomeration of MH NPs was obstructed by the 3D nanoporous structure of cellulose aerogel, which played as a good scaffold/template for the nucleation and growth of MH NPs.[25] According to the aforementioned results, MH NPs@cellulose composite aerogels with a homogeneous nanoporous structure can be fabricated via in situ templated synthesis of MH NPs in the cellulose gel scaffold.

The nanostructure of the MH NPs@cellulose composite aerogel was further examined by TEM and EDS analysis. As shown in Figure 4, MH NPs, which can be clearly observed Figure S2, Supporting Information, are evenly distributed in the cellulose matrix. In addition, EDS spectra show that the main elements in the composite aerogel are Mg, C, and O. The peak at ca. 8 eV can be assigned to the peak of Cu[26] because the sample was deposited on the copper grid for TEM observation. This result demonstrates the successful formation and good dispersion of MH NPs in the composite aerogel, which is consistent with the XRD result.

To further investigate the pore structure of the aerogels, nitrogen adsorption and desorption isotherm techniques were conducted. Figure 5a shows the adsorption and desorption

DOI: 10.1021/acssuschemeng.5b00438
ACS Sustainable Chem. Eng. 2015, 3, 1853−1859

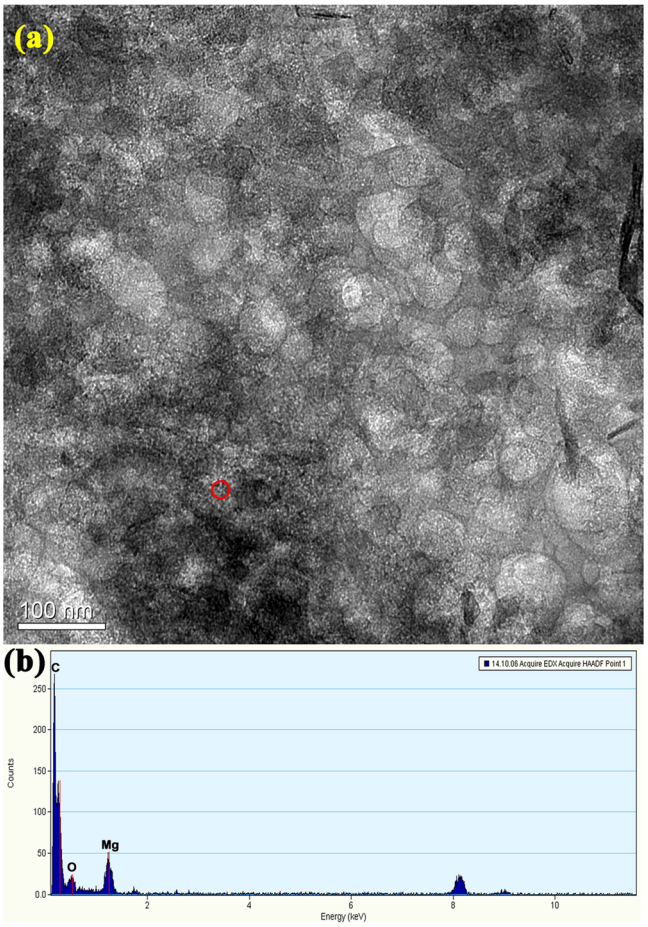

Figure 4. TEM image (a) and EDS spectra (b) of MH NPs@cellulose composite aerogel (CA2).

isotherms, which exhibit a hysteresis typical of a porous system. No distinct changes in the shape of isotherms and N_2 adsorption amount could be observed in the isotherms. According to Brunauer–Emmett–Teller (BET) analysis, a total specific surface area of 38.8 and 37.6 $m^2\ g^{-1}$ are obtained for the neat cellulose aerogel and MH NPs@cellulose composite aerogel, respectively. Additionally, the pure cellulose aerogel only exhibits one peak at 33 nm as shown in Figure 5b, while the MH@cellulose composite aerogel shows two peaks at 33 and 13 nm. The peaks at 33 nm of pure cellulose aerogel as well as MH@cellulose composite aerogel arise from the cellulose network structure in aerogels. The sharp peak at 13 nm of the MH@cellulose composite aerogel can be attributed to the finer structure due to the incorporation of MH NPs into the cellulose network structure.[27] The results indicate that the incorporation of MH NPs into the cellulose aerogel did not significantly block or result in the collapse of its porous structure, which is in accordance with the morphology observation.

Heat Insulation Performance of MH NPs@Cellulose Composite Aerogels. To evaluate the heat insulation performance, the transient plane source (TPS) method was used to measure the thermal conductivity. As the main factors to affect the heat insulation property of materials, the density and porosity of aerogels are measured and shown in Figure 6a and b.[28] The neat cellulose aerogel has a low density and high porosity. As a result, the thermal conductivity of neat cellulose aerogel is only 0.056 W $m^{-1}\ k^{-1}$ (Figure 6c). With the increased content of MH NPs, the density increases while the porosity shows a slight decrease. Meanwhile, the thermal conductivity of aerogels increases. Generally, the thermal conductivity of dense solid is always higher than that of still air. At normal temperatures, the increase in solid matter content in unit volume leads to higher thermal conductivity, while an increase in porosity can restrict the propagation of phonon in aerogels,[29] which results in a better heat insulation property. In the case of MH NPs@cellulose aerogels, due to the introduction of MH into cellulose, MH NPs@cellulose aerogels exhibited higher density and lower porosity, thus resulting in higher thermal conductivity when compared to pure cellulose aerogel. However, the highest thermal conductivity of the composite aerogels (CA4) is 0.081 W $m^{-1}\ k^{-1}$, which is still at a lower level. Hence, the thermal conductivity of MH NPs@cellulose composite aerogels have changes slightly with the introduction of MH NPs.

Mechanical Properties of MH NPs@Cellulose Composite Aerogels. Good mechanical strength is essential for heat

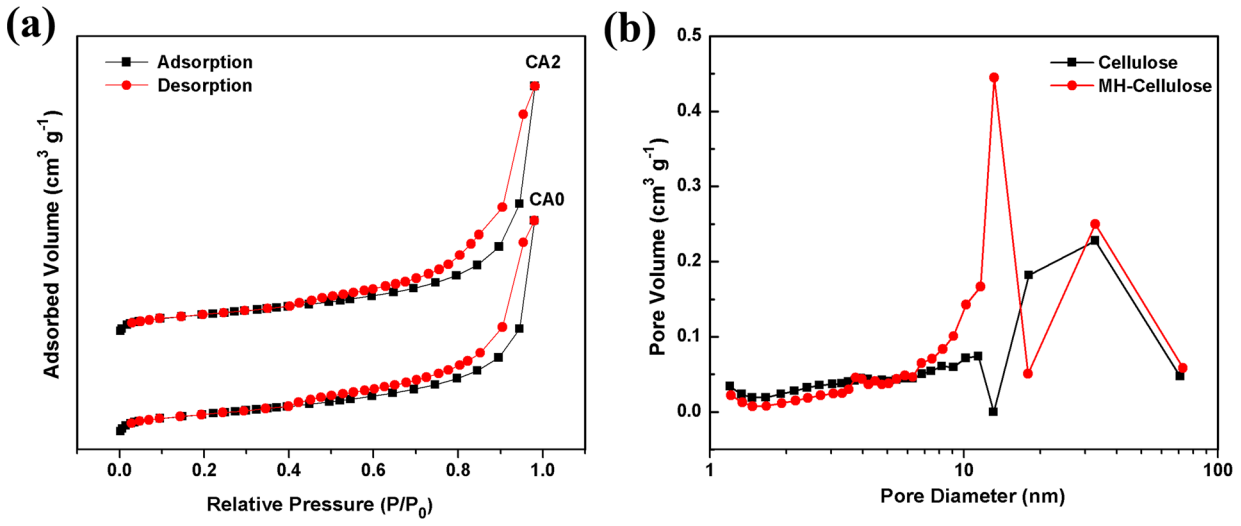

Figure 5. Nitrogen adsorption and desorption isotherms (a) and BJH pore size distribution (b) of neat cellulose aerogel and MH NPs@cellulose composite aerogel (CA2).

DOI: 10.1021/acssuschemeng.5b00438
ACS Sustainable Chem. Eng. 2015, 3, 1853–1859

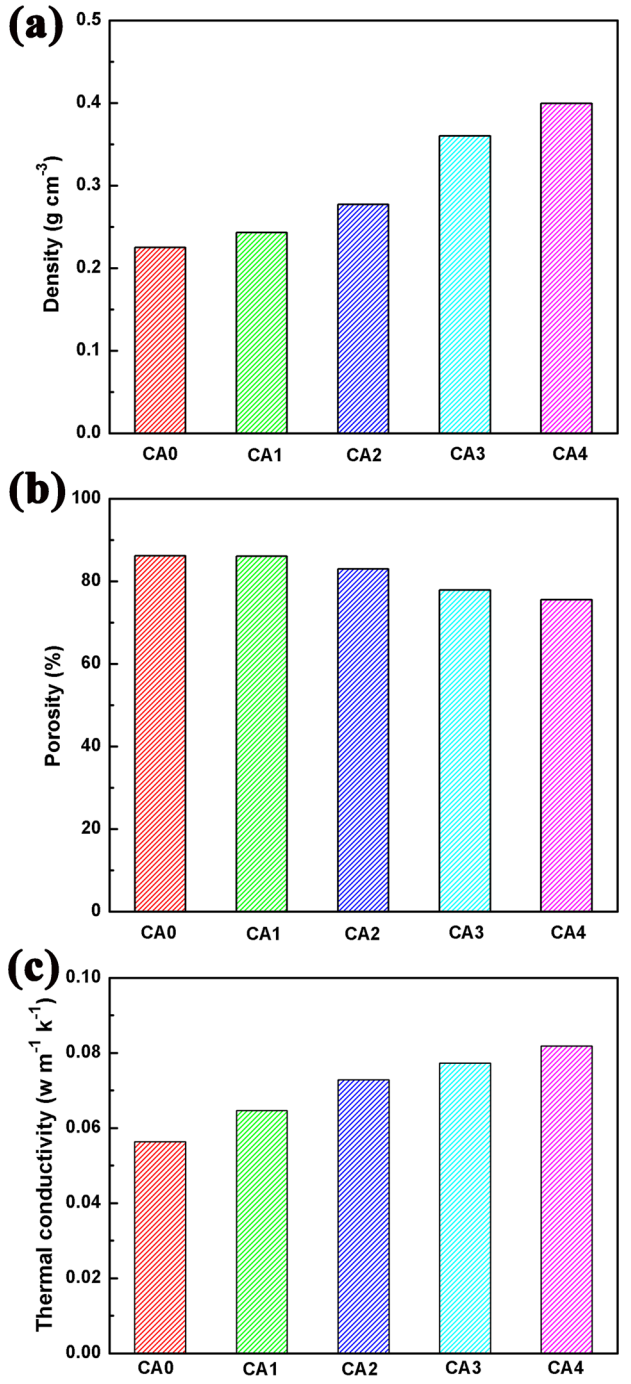

Figure 6. Density (a), porosity (b), and thermal conductivity (c) of aerogels as a function of MH NPs content.

insulating materials. The compressive stress−strain curves of the composite aerogels are shown in Figure 7a. At the beginning of stress−strain curves, the upward trend is very slow and then rises sharply, indicating ideal compressive strength.[30] Obviously, the compressive strength increases with the increment of MH NPs content (Figure 7b). For the neat cellulose aerogel, the compressive strength is 141 KPa, while for the composite aerogel CA4, the compressive strength is 467 KPa, enhanced by 231.2%. The compressive strength of the MH NPs@cellulose composite aerogel is much higher than that of the neat cellulose aerogel. These results reveal that the MH NPs play an important role in the improvement of the mechanical strength of cellulose aerogel. This could be because the introduction of MH NPs make a more condensed structure to avoid collapse of the three-dimensionally nanoporous structures of cellulose aerogels, resulting in a higher compressive strength. Because of the enhanced compressive strength, the MH NPs@cellulose composite aerogels are potentially useful as heat insulating material with high mechanical strength.

Flame Retardancy of MH NPs@Cellulose Composite Aerogels. In order to investigate the flame retardancy performance of the composite aerogels, the aerogels were ignited and the combustion velocity was calculated. In this case, the neat cellulose aerogel was ignited quickly with rapid flame propagation and burned completely after 10 s of combustion (see the video in Supporting Information). However, the MH NPs@cellulose composite aerogels still remained to some extent after 10 s of burning, and the residual length did not change notably among CA2, CA3, and CA4 (Figure 8a,b). The digital photo in Figure 8c shows the residues of the CA2 after self-extinguishing. With an increase in MH NPs content, the combustion velocity of aerogels decreases from 5 to 0.8 mm s^{-1} (Figure 8c). The results indicate that the incorporation of MH NPs could efficiently increase the flame retardancy of the cellulose aerogel. It is interesting to note that the composite aerogels self-extinguished when the MH NPs content reached 82 phr. When the CA2 was ignited, flame propagation apparently slowed, and then the flame gradually became smaller and finally extinguished within 40 s (see the video in Supporting Information). The results indicate that the addition of MH NPs endowed the cellulose aerogel with good flame retardant properties.

Thermal Stability of MH NPs@Cellulose Composite Aerogels. In view of the importance of thermal stability for the practical application of heat insulating materials, the thermal decomposition of the composite aerogel was investigated by TGA analysis and compared with the neat cellulose aerogel. As shown in Figure 9, a slight weight loss occurs at relatively low temperature (<100 °C) for both of the samples due to the loss of moisture. The stage of weight loss around 314.2−371.0 °C can be attributed to the depolymerization of cellulose with generation of CO_2 and volatile hydrocarbons. The starting decomposition temperature of the MH NPs@cellulose composite aerogel is lower than that of the neat cellulose aerogel. This may be attributed to the decomposition of MH NPs, which undergoes decomposition at lower temperature than ordinary magnesium hydroxide.[31,32] The maximum decomposition temperature of the composite aerogel is 353.3 °C and that of the neat cellulose aerogel is 349.9 °C. As a result, the thermostability of aerogels did not change significantly with the incorporation of MH NPs.

CONCLUSIONS

MH NPs@cellulose composite aerogels with a homogeneous nanoporous structure were fabricated successfully from waste cotton fabrics via in situ templated synthesis of MH NPs in the cellulose gel scaffold. This is a simple, low cost, efficient, and environmentally friendly process to realize fine dispersion of flame retardants in cellulose aerogel and avoid collapse of its nanoporous structure. The as-prepared composite aerogels still have highly porous networks and excellent heat insulation performance with the low thermal conductivity. Besides, the composite aerogels exhibit good flame retardant properties and mechanical properties. This environmentally friendly and low

DOI: 10.1021/acssuschemeng.5b00438
ACS Sustainable Chem. Eng. 2015, 3, 1853−1859

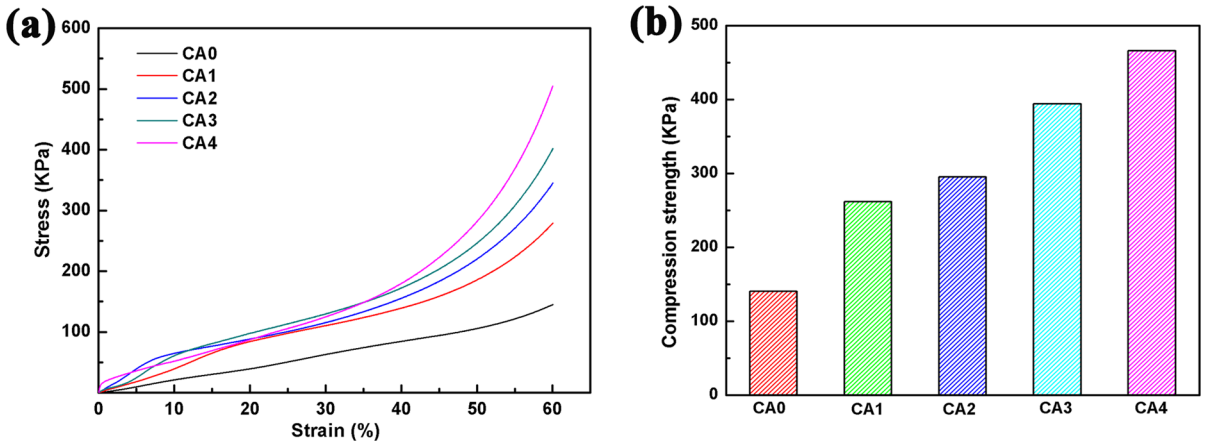

Figure 7. Compression stress−strain curves (a) and compressive strength (b) of aerogels.

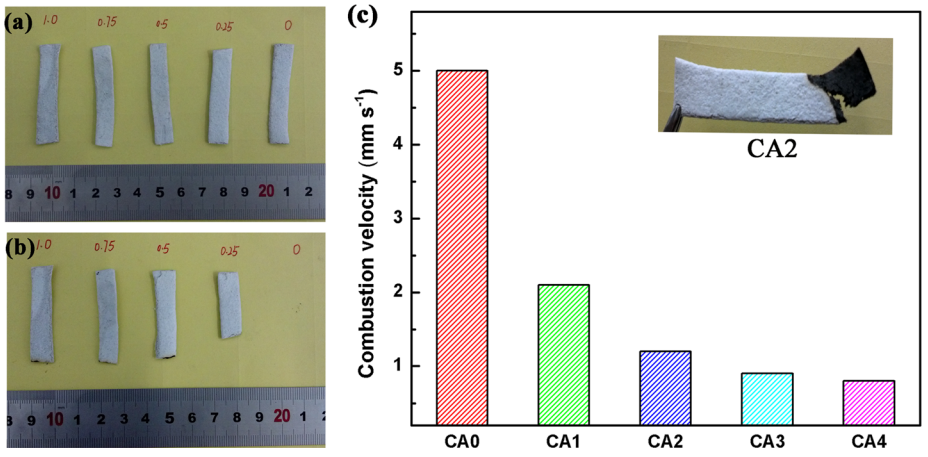

Figure 8. Digital photographs of original aerogels before (a) and after (b) 10 s of combustion. Combustion velocity as a function of MH NPs content (c).

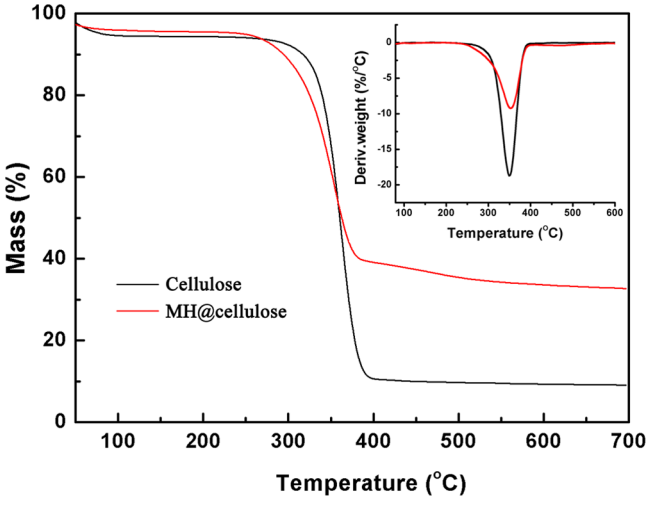

Figure 9. TGA and DTG curves of neat cellulose aerogel and MH NPs@cellulose composite aerogel (CA2).

cost process opens new opportunities for the use of inexpensive waste-derived cellulose to fabricate heat insulating materials. It may be suitable for industrial scale production and has a great potential application in the future of green building materials.

■ ASSOCIATED CONTENT

Supporting Information

SEM image and EDS spectra of MH NPs@cellulose composite aerogel. TEM image of MH NPs@cellulose composite aerogel. Videos of combustion of neat cellulose aerogel and MH@cellulose composite aerogel. The Supporting Information is available free of charge on the ACS Publications website at DOI: 10.1021/acssuschemeng.5b00438.

■ AUTHOR INFORMATION

Corresponding Authors

*E-mail: xxzwwh@scu.edu.cn. Tel: +86-28-85460607. Fax: +86-28-85402465. (X. Zhang).

*E-mail: canhuilu@scu.edu.cn. Tel: +86-28-85460607. Fax: +86-28-85402465. (C. Lu).

Notes

The authors declare no competing financial interest.

■ ACKNOWLEDGMENTS

The authors thank the National Science Foundation of China (51203105 and 51473100) and State Key Laboratory of Polymer Materials Engineering (Grant sklpme2015-3-04) for financial support.

DOI: 10.1021/acssuschemeng.5b00438
ACS Sustainable Chem. Eng. 2015, 3, 1853−1859

REFERENCES

(1) He, X.; Zhang, X.; Zhang, W.; Tian, D.; Lu, C. Mechanochemically activated waste-derived cellulose as a novel functional additive to enhance melt processability and mechanical properties of poly(vinyl alcohol). *J. Vinyl Addit. Technol.* **2014**, *20*, 177−184.

(2) Miranda, R.; Sosa-Blanco, C.; Bustos-Martínez, D.; Vasile, C. Pyrolysis of textile wastes: I. Kinetics and yields. *J. Anal. Appl. Pyrolysis* **2007**, *80*, 489−495.

(3) Huang, F.; Xu, Y.; Peng, B.; Su, Y.; Jiang, F.; Hsieh, Y. L.; Wei, Q. Coaxial electrospun cellulose-core fluoropolymer-shell fibrous membrane from recycled cigarette filter as separator for high performance lithium-ion battery. *ACS Sustainable Chem. Eng.* **2015**, *3*, 932−940.

(4) Lam, E.; Leung, A. C. W.; Liu, Y.; Majid, E.; Hrapovic, S.; Male, K. B.; Luong, J. H. T. Green strategy guided by Raman spectroscopy for the synthesis of ammonium carboxylated nanocrystalline cellulose and the recovery of byproducts. *ACS Sustainable Chem. Eng.* **2013**, *1*, 278−283.

(5) Salam, A.; Lucia, L. A.; Jameel, H. A novel cellulose nanocrystals-based approach to improve the mechanical properties of recycled paper. *ACS Sustainable Chem. Eng.* **2013**, *1*, 1584−1592.

(6) Ratanakamnuan, U.; Atong, D.; Aht-Ong, D. Cellulose esters from waste cotton fabric via conventional and microwave heating. *Carbohydr. Polym.* **2012**, *87*, 84−94.

(7) Tian, D.; Zhang, X.; Lu, C. Solvent-free synthesis of carboxylate-functionalized cellulose from waste cotton fabrics for the removal of cationic dyes from aqueous solutions. *Cellulose* **2014**, *21*, 473−484.

(8) Sun, X.; Lu, C.; Liu, Y.; Zhang, W.; Zhang, X. Melt-processed poly(vinyl alcohol) composites filled with microcrystalline cellulose from waste cotton fabrics. *Carbohydr. Polym.* **2014**, *101*, 642−649.

(9) Hong, F.; Guo, X.; Zhang, S.; Han, S.; Yang, G.; Jönsson, L. Bacterial cellulose production from cotton-based waste textiles: Enzymatic saccharification enhanced by ionic liquid pretreatment. *Bioresour. Technol.* **2012**, *104*, 503−508.

(10) Cuce, E.; Cuce, P.; Wood, C. J.; Riffat, S. B. Toward aerogel based thermal superinsulation in buildings: A comprehensive review. *Renewable Sustainable Energy Rev.* **2014**, *34*, 273−299.

(11) Cai, J.; Liu, S.; Feng, J.; Kimura, S.; Wada, M.; Kuga, S.; Zhang, L. Cellulose-silica nanocomposite aerogels by in situ formation of silica in cellulose gel. *Angew. Chem., Int. Ed.* **2012**, *51*, 2076−2079.

(12) Cai, J.; Zhang, L. Unique gelation behavior of cellulose in NaOH/Urea aqueous solution. *Biomacromolecules* **2006**, *7*, 183−189.

(13) Qi, H.; Mäder, E.; Liu, J. Electrically conductive aerogels composed of cellulose and carbon nanotubes. *J. Mater. Chem. A* **2013**, *1*, 9714−9720.

(14) Zhou, Z.; Zhang, X.; Lu, H.; Lan, L.; Yuan, G. Polyaniline-decorated cellulose aerogel nanocomposite with strong interfacial adhesion and enhanced photocatalytic activity. *RSC Adv.* **2014**, *4*, 8966−8972.

(15) Chin, S. F.; Romainor, A. N. B.; Pang, S. C. Fabrication of hydrophobic and magnetic cellulose aerogel with high oil absorption capacity. *Mater. Lett.* **2014**, *115*, 241−243.

(16) Li, Y. Q.; Samad, Y. A.; Polychronopoulou, K.; Alhassan, S. M.; Liao, K. Carbon aerogel from winter melon for highly efficient and recyclable oils and organic solvents absorption. *ACS Sustainable Chem. Eng.* **2014**, *2*, 1492−1497.

(17) Sadineni, S.; Madala, S.; Boehm, R. Passive building energy savings: A review of building envelope components. *Renewable Sustainable Energy Rev.* **2011**, *15*, 3617−3631.

(18) Olsson, R. T.; Azizi Samir, M. A. S.; Salazar-Alvarez, G.; Belova, L.; Ström, V.; Berglund, L. A.; Ikkala, O.; Nogués, J.; Gedde, U. W. Making flexible magnetic aerogels and stiff magnetic nanopaper using cellulose nanofibrils as templates. *Nat. Nanotechnol.* **2010**, *5*, 584−588.

(19) Hosoda, N.; Tsujimoto, T.; Uyama, H. Green composite of Poly(3-hydroxybutyrate-co-3-hydroxyhexanoate) reinforced with porous cellulose. *ACS Sustainable Chem. Eng.* **2014**, *2*, 248−253.

(20) Xiong, R.; Lu, C.; Wang, Y.; Zhou, Z.; Zhang, X. Nanofibrillated cellulose as the support and reductant for the facile synthesis of Fe_3O_4/Ag nanocomposites with catalytic and antibacterial activity. *J. Mater. Chem. A* **2013**, *1*, 14910−14918.

(21) Huang, H. D.; Liu, C. Y.; Zhang, L. Q.; Zhong, G. J.; Li, Z. M. Simultaneous reinforcement and toughening of carbon nanotube/cellulose conductive nanocomposite films by interfacial hydrogen bonding. *ACS Sustainable Chem. Eng.* **2015**, *3*, 317−324.

(22) Huang, H. D.; Liu, C. Y.; Zhou, D.; Jiang, X.; Zhong, G. J.; Yan, D. X.; Li, Z. M. Cellulose composite aerogel for highly efficient electromagnetic interference shielding. *J. Mater. Chem. A* **2015**, *3*, 4983−4991.

(23) Qi, H.; Cai, J.; Zhang, L.; Kuga, S. Properties of films composed of cellulose nanowhiskers and a cellulose matrix regenerated from alkali/urea solution. *Biomacromolecules* **2009**, *10*, 1597−1602.

(24) Ding, Y.; Zhang, G.; Wu, H.; Hai, B.; Wang, L.; Qian, Y. Nanoscale magnesium hydroxide and magnesium oxide powders: control over size, shape, and structure via hydrothermal synthesis. *Chem. Mater.* **2001**, *13*, 435−440.

(25) Chen, L.; Cao, W.; Quinlan, P. J.; Berry, R. M.; Tam, K. C. Sustainable catalysts from gold-loaded polyamidoamine dendrimer-cellulose nanocrystals. *ACS Sustainable Chem. Eng.* **2015**, *3*, 978−985.

(26) Wu, X.; Lu, C.; Zhang, W.; Yuan, G.; Xiong, R.; Zhang, X. A novel reagentless approach for synthesizing cellulose nanocrystal-supported palladium nanoparticles with enhanced catalytic performance. *J. Mater. Chem. A* **2013**, *1*, 8645−8652.

(27) Yu, J.; Xu, A.; Zhang, L.; Song, R.; Wu, L. Synthesis and characterization of porous magnesium hydroxide and oxide nanoplates. *J. Phys. Chem. B* **2004**, *108*, 64−70.

(28) Shi, J.; Lu, L.; Guo, W.; Sun, Y.; Cao, Y. An environment-friendly thermal insulation material from cellulose and plasma modification. *J. Appl. Polym. Sci.* **2013**, *130*, 3652−3658.

(29) Lu, X.; Caps, R.; Fricke, J.; Alviso, C. T.; Pekala, R. W. Correlation between structure and thermal conductivity of organic aerogels. *J. Non-Cryst. Solids* **1995**, *188*, 226−234.

(30) Shi, X.; Hu, Y.; Tu, K.; Zhang, L.; Wang, H.; Xu, J.; Zhang, H.; Li, J.; Wang, X.; Xu, M. Electromechanical polyaniline-cellulose hydrogels with high compressive strength. *Soft Matter* **2013**, *9*, 10129−10134.

(31) Yu, J.; Xu, A.; Zhang, L.; Song, R.; Wu, L. Synthesis and characterization of porous magnesium hydroxide and oxide nanoplates. *J. Phys. Chem. B* **2004**, *108*, 64−70.

(32) Shkatulov, A.; Ryu, J.; Kato, Y.; Aristov, Y. Composite material "$Mg(OH)_2$/vermiculite": A promising new candidate for storage of middle temperature heat. *Energy* **2012**, *44*, 1028−1034.

DOI: 10.1021/acssuschemeng.5b00438
ACS Sustainable Chem. Eng. 2015, 3, 1853−1859